Article

Neuron

Network Dynamics Mediate Circadian Clock Plasticity

Highlights

- Circadian phasing of SCN subregions is stably altered by light:dark cycle length
- Changes in DNA methylation are region specific and necessary for network changes
- SCN network reorganization requires GABAergic signaling
- Interruption of neural communication abolishes circadian aftereffects of altered light

Authors

Abdelhalim Azzi, Jennifer A. Evans, Tanya Leise, Jihwan Myung, Toru Takumi, Alec J. Davidson, Steven A. Brown

Correspondence

jennifer.evans@marquette.edu (J.A.E.), adavidson@msm.edu (A.J.D.), steven.brown@pharma.uzh.ch (S.A.B.)

In Brief

Altered light exposure stably changes the period of daily rhythms. This change in period is driven epigenetically, not by changes in the clock properties of individual cells, but by changes in neural communication among clock cells.

Accession Numbers

GSE89255

Azzi et al., 2017, Neuron *93*, 441–450
January 18, 2017
http://dx.doi.org/10.1016/j.neuron.2016.12.022

CellPress

Neuron
Article

Network Dynamics Mediate Circadian Clock Plasticity

Abdelhalim Azzi,[1,6] Jennifer A. Evans,[2,6,*] Tanya Leise,[3] Jihwan Myung,[4] Toru Takumi,[4] Alec J. Davidson,[5,*] and Steven A. Brown[1,7,*]

[1]Institute of Pharmacology and Toxicology, University of Zurich, Winterthurerstrasse 190, 8057 Zürich, Switzerland
[2]Department of Biomedical Sciences, College of Health Sciences, Marquette University, 1250 W. Wisconsin Ave., Milwaukee, WI 53233, USA
[3]Department of Mathematics and Statistics, Amherst College, 220 S. Pleasant St., Amherst, MA 01002, USA
[4]RIKEN Brain Science Institute (BSI), 2-1 Hirosawa Wako City, Saitama 351-0198, Japan
[5]Department of Neurobiology, Morehouse School of Medicine, 720 Westview Dr., Atlanta, GA 30310, USA
[6]Co-first author
[7]Lead Contact
*Correspondence: jennifer.evans@marquette.edu (J.A.E.), adavidson@msm.edu (A.J.D.), steven.brown@pharma.uzh.ch (S.A.B.)
http://dx.doi.org/10.1016/j.neuron.2016.12.022

SUMMARY

A circadian clock governs most aspects of mammalian behavior. Although its properties are in part genetically determined, altered light-dark environment can change circadian period length through a mechanism requiring de novo DNA methylation. We show here that this mechanism is mediated not via cell-autonomous clock properties, but rather through altered networking within the suprachiasmatic nuclei (SCN), the circadian "master clock," which is DNA methylated in region-specific manner. DNA methylation is necessary to temporally reorganize circadian phasing among SCN neurons, which in turn changes the period length of the network as a whole. Interruption of neural communication by inhibiting neuronal firing or by physical cutting suppresses both SCN reorganization and period changes. Mathematical modeling suggests, and experiments confirm, that this SCN reorganization depends upon GABAergic signaling. Our results therefore show that basic circadian clock properties are governed by dynamic interactions among SCN neurons, with neuroadaptations in network function driven by the environment.

INTRODUCTION

Neurons in many parts of the brain show functional adaptations in response to the signals they receive. Such neuroplasticity is the basis not only for memory, but for numerous other cognitive and emotional responses (Marsden, 2013). As in higher-order cognitive function, the process of biological timing is also markedly plastic. However, the mechanisms of this plasticity remain mostly unexplored.

Circadian clocks control and synchronize most behavioral and physiological processes of the organism to the 24 hr solar day. The fundamental unit of circadian timing is cell autonomous: at the molecular level, circadian clocks are based primarily upon interconnected transcription-translation feedback loops that function within nearly every cell of the body. Anatomically, these clocks are hierarchically organized under a master clock located in the suprachiasmatic nuclei (SCN) of the hypothalamus, a network of several thousand neural clock cells (Brown and Azzi, 2013). SCN neurons are divided into at least two distinct populations—a ventral (vSCN) "core" region that receives retinal projections, and a dorsal (dSCN) "shell" that projects to other brain areas (Antle and Silver, 2005). These regions form a circuit that is locally and regionally coupled via multiple signaling mechanisms (Aton and Herzog, 2005) that confer robustness and precision to the SCN clock mechanism (Abraham et al., 2010; Herzog et al., 2004; Liu et al., 2007).

Genetic alterations of clock properties at the molecular level produce corresponding changes in daily behavioral rhythms (Lowrey et al., 2000; Toh et al., 2001), which have been localized to the SCN rather than elsewhere in the brain or body (Low-Zeddies and Takahashi, 2001; Ralph et al., 1990). Epigenetic changes are similarly possible: we and others have shown previously that exposing genetically identical mice to non-24 hr light:dark cycles ("Zeitgeber periods," Aschoff and Pohl, 1978) results in stable changes of endogenous free-running period lasting several months, termed "aftereffects" (Pittendrigh and Daan, 1976), which depend on dynamic DNA methylation in SCN cells (Azzi et al., 2014). Plasticity in circadian period appears to be a conserved property of the mammalian timing system, as similar behavioral effects have been observed in humans (Scheer et al., 2007). Effects of other changes in light-dark cycle, such as changes in the proportion of light and dark within the 24 hr day (photoperiod, which is seasonally variant in nature) or erratic light-dark cycles, have also been examined. For example, DNA methylation also plays an important role in regulating seasonal endocrine changes (Stevenson and Prendergast, 2013). However, unlike the "zeitgeber periods" mentioned above, neither photoperiod nor erratic light-dark cycles have shown significant long-lasting period aftereffects (Pittendrigh and Daan, 1976).

In rodents, SCN function has been studied using ex vivo systems, where changes in clock properties are revealed using real-time fluorescence or bioluminescence monitoring of SCN slices from transgenic rodents: PER1:GFP (Kriegsfeld et al., 2003), *Per1-luc* (Stokkan et al., 2001), *Bmal1-luc* (Nakajima et al., 2010; Nishide et al., 2006), and PER2::LUC mice (Pendergast

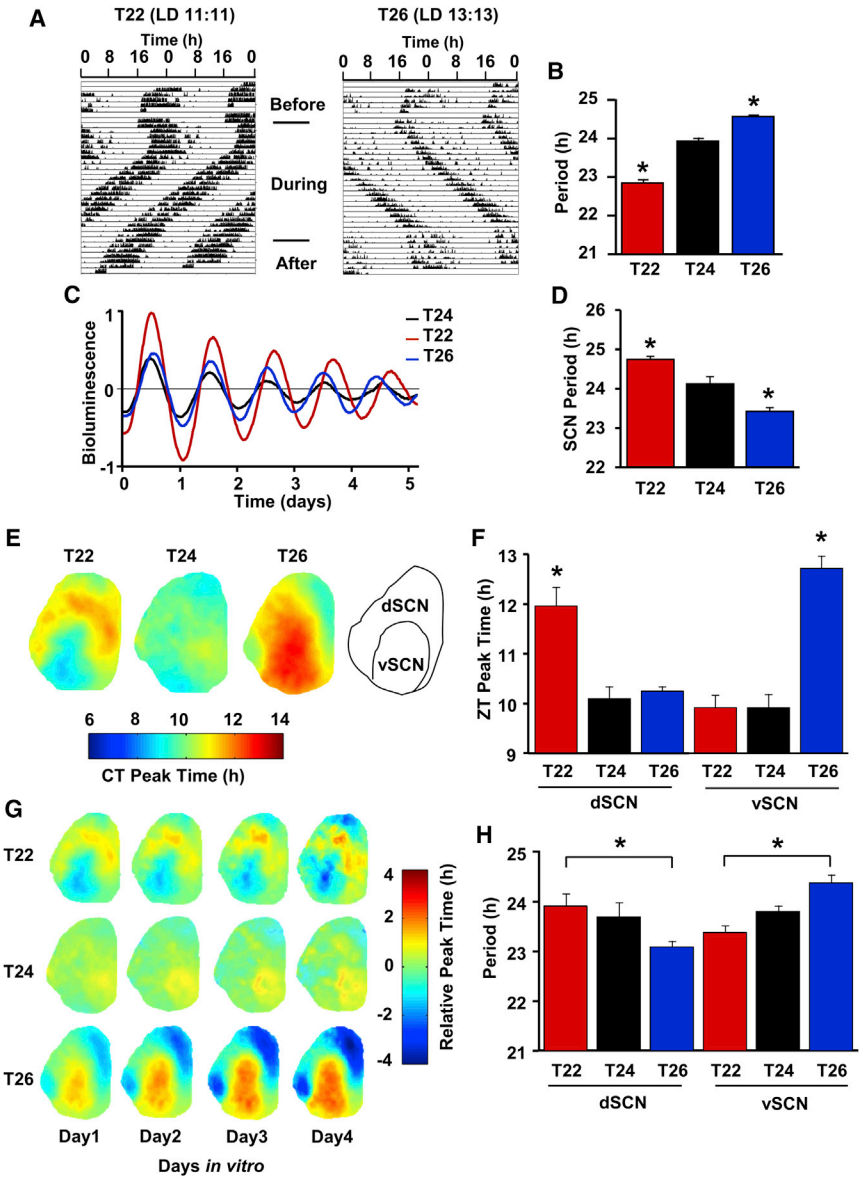

Figure 1. Altered Light:Dark Cycle Length Changes Circadian Behavior and SCN Topology

See also Figures S1–S3.

(A) Actograms of wheel running for representative PER2::LUC mice before, during, and after entrainment to light:dark cycle lengths of 22 and 26 hr (T22, T26).

(B) Free-running period (mean ± SEM, here and elsewhere) after entrainment. (n = 4–10/group, 1w-ANOVA $F(2,21) = 135.51$, $p < 0.0001$, * Dunnett's post hoc test, $p < 0.05$).

(C) PER2::LUC bioluminescence intensity (detrended bioluminescence relative to maximum) in representative SCN slices from mice entrained to different light:dark cycles.

(D) Bar graph of data in (C), n = 5–7 slices/group. 1w-ANOVA $F(2,12) = 37.89$, $p < 0.0001$; * Tukey's HSD test post hoc test $p < 0.01$.

(E) Average phase maps for SCN after entrainment to T22, T24, and T26, illustrating regional differences in the circadian time (CT) of peak PER2::LUC expression on the first day in vitro. n = 9–10/group.

(F) Quantification of average CT peak time on the first cycle in vitro for dorsal SCN (dSCN) and ventral SCN (vSCN), as illustrated in (E). dSCN: 1w-ANOVA $F(2,28) = 15.89$, $p < 0.0001$; vSCN: 1w-ANOVA $F(2,28) = 37.58$, $p < 0.0001$; * Dunnett's post hoc test, $p < 0.05$.

(G) Average phase maps illustrating changes in regional phase over the first 4 days in vitro for SCN from T22, T24, and T26 mice. Color scale shows the time of peak PER2::LUC relative to that for the field rhythm of the whole slice. n = 9–10/cycle/group.

(H) Average period of dSCN and vSCN regions, quantified from data in (G). dSCN: 1w-ANOVA $F(2,28) = 4.36$, $p < 0.05$; vSCN: 1w-ANOVA $F(2,28) = 4.56$, $p < 0.05$; * Tukey's HSD test, $p < 0.05$. Errors bars are mean ± SE.

et al., 2010; Yoo et al., 2004) each have reporter gene expression timed by endogenous clock properties. The topology of SCN networks examined with these tools shows remarkable plasticity. For example, we and others have shown that the molecular clocks of SCN neurons change their phase in a region-specific manner after changes in the light:dark cycle (Evans et al., 2013; Nagano et al., 2003; Nakamura et al., 2005; Sellix et al., 2012). The circadian period length in SCN slices normally correlates tightly with behavioral period length (Liu et al., 1997; Yoo et al., 2004; Myung et al., 2012). Surprisingly, however, in the case of altered day-night period (light:dark cycle length longer or shorter than 24 hr), the period length of SCN slices shows an inverse correlation with behavioral period (Aton et al., 2004; Molyneux et al., 2008). To date, changes in light:dark cycle length remain the only entrainment condition that causes a dramatic mismatch between ex vivo and in vivo rhythms.

Here, we report that SCN regional coupling is dynamically modulated to reprogram global clock properties, providing a mechanism for this mismatch as well as a surprising and elegant epigenetic path by which the local environment can stably alter SCN period. This mechanism could provide a paradigm for understanding other forms of environment-related changes in behavior.

RESULTS

Altered Light:Dark Cycle Length Temporally Reorganizes the SCN Network

Male PER2::LUC mice (Yoo et al., 2004) were entrained to light:dark cycles either 22, 24, or 26 hr in length (T22, T24, or T26) for 6 weeks. Daily rhythms were influenced by cycle length in a manner consistent with previous work (Pittendrigh and Daan, 1976). Notably, upon release into constant darkness, T22 mice displayed free-running rhythms with the shortest period, whereas T26 mice had the longest period (Figures 1A and 1B).

Further, the timing of entrained rhythms was altered by cycle length, with T22 mice displaying the latest times of activity onset and T26 mice the earliest (Figures S1A and S1B), which is also expected (Pittendrigh and Daan, 1976). To directly investigate the neural basis of these period aftereffects, we collected SCN slices from T22-, T24-, and T26-entrained mice for ex vivo real-time bioluminometry. In these SCN slices, the inverse correlation described above is evident between period length in vivo and ex vivo (Figures 1C and 1D), as reported previously (Aton et al., 2004; Molyneux et al., 2008). The effect was specific to the SCN because peripheral tissues such as the liver did not display PER2::LUC rhythms with an inverse period aftereffect (Figure S1C; Molyneux et al., 2008).

The observation that the circadian periods at the behavioral and neural levels do not match is inconsistent with the long-held theory that cell-autonomous circadian period of SCN cells determines behavioral period (Herzog et al., 1998; Low-Zeddies and Takahashi, 2001; Ralph et al., 1990). Therefore, we next used real-time bioluminescence imaging to investigate the impact of cycle length on the spatiotemporal function of the SCN network. Cycle length induced a clear phase separation among SCN sub-regions that was organized in complementary manner in T22 versus T26 (Figures 1E and 1F). Relative to the dSCN, the phase of PER2::LUC rhythms in the vSCN was significantly earlier in T22, but later in T26 (Figures 1E and 1F). Similar cycle-induced changes in regional phase were evident throughout the rostrocaudal SCN (Figure S2A). Surprisingly, regional phase differences became more pronounced each successive day in vitro (Figure 1G), suggesting that cycle length altered period in a region-specific manner (Figure 1H). In cultured SCN slices, vSCN showed a shorter period in T22 than in T26 ($p = 0.02$), whereas dSCN showed a shorter period in T26 than in T22 ($p = 0.02$) (Figure 1H). In T24, both periods were around 24 hr, and phase differences were less pronounced (Figure 1H). Therefore, in SCN slices, the period of the vSCN subregion showed a positive correlation with cycle length, whereas the dSCN showed a negative relationship with cycle length (Figure S3). Thus, the inverse period aftereffect is a region-specific feature of the SCN network, with the period of the dSCN likely dominating the period of field rhythm of the whole slice measured with luminometry (Figures 1C and 1D) due to its relatively larger size and stronger bioluminescence signals (Figure S2B).

Light:Dark Cycle Length Drives Region-Specific Methylation Changes

We have previously demonstrated that different light:dark cycle lengths result in dynamic changes in DNA methylation within the SCN that globally alter transcription of both clock genes and non-clock genes (Azzi et al., 2014). Given that light:dark cycle length produces region-specific changes in phase, we decided to re-examine DNA methylation in the SCN separately for dorsal and ventral regions. Consistent with the phase polarization observed in Figure 1, in fact different sets of genes showed methylation changes in dorsal versus ventral regions (Figures 2A and 2B). Far greater changes were observed in vSCN than in dSCN (Figures 2A and 2B; $p < 0.001$), which makes sense because of the innervation of vSCN by the retinohypothalamic tract, the source of light input (Hannibal and Fahrenkrug, 2004; Lokshin et al., 2015). Hierarchical clustering showed that whereas DNA methylation in the dSCN under different cycle lengths formed one cluster, methylation in the vSCN formed a second more diverged cluster (Figure 2C). Examining the families of genes whose methylations were altered, the most significant categories were neurotransmitter receptors and ion channels (Figure 3), each represented by a family of multiple genes including several potassium, calcium, and GABA channels (Figures S4 and S5). Collectively, these ontological analyses reinforce the idea that altered light:dark cycles might change networking within the SCN.

SCN Interregional Communication Drives Aftereffects

As demonstrated by many labs, the period length of a circadian oscillator determines its phase under entrained conditions (Brown et al., 2008). To explain our data, the easiest explanation would therefore be that cellular epigenetic changes altered cellular period lengths, especially within vSCN, thereby driving phase differences. To test this hypothesis, we prepared SCN coronal slices from mice entrained to T22, T24, and T26, and then using a surgical knife, we physically separated SCN slices into approximate vSCN and dSCN regions. Unexpectedly, periods of the physically separated SCN sub-regions did not show significant differences relative to each other or among the three conditions of T22, T24, and T26 (Figures 4A and 4B). This result suggested that the changes in SCN period documented above were not mediated by region-specific changes in cellular period, but rather by changes dependent upon communication between SCN sub-regions.

Action potentials and neuropeptides are the main signals exchanged among SCN neurons (Albus et al., 2005; Aton et al., 2005; Harmar et al., 2002). To directly examine the role of intra-network signaling in determining cycle-related changes in period, we cultured coronal SCN slices of T22, T24, and T26 mice in the presence or absence of 2 μM of tetrodotoxin (TTX) to block voltage-gated sodium channels (Noda et al., 1986), and thereby inhibited the firing of action potentials and the synaptic release of SCN coupling factors (Earnest et al., 1991). Consistent with a primary role for neural communication rather than cell-autonomous clock properties in driving cycle length-dependent period changes, blocking synaptic communication with TTX induced SCN period relaxation to the inverse of what was observed in its absence (Figures 4C and 4D). Concomitantly, region-specific differences in both period and phase in SCN slices from T22 and T26 animals were relaxed (Figures 4E and 4F).

Mathematical Modeling Predicts a Role for GABA Signaling

To investigate how plasticity in regional coupling could drive the observed effects of cycle length on period, we created a mathematical model in which vSCN and dSCN oscillators are connected via two complementary coupling mechanisms that have been revealed experimentally: one mechanism that synchronizes oscillators and another mechanism that desynchronizes oscillators close in phase (Evans et al., 2013; Freeman et al., 2013a) (Figure 5A). The relative strengths of the two coupling mechanisms in the model depend on the cycle length,

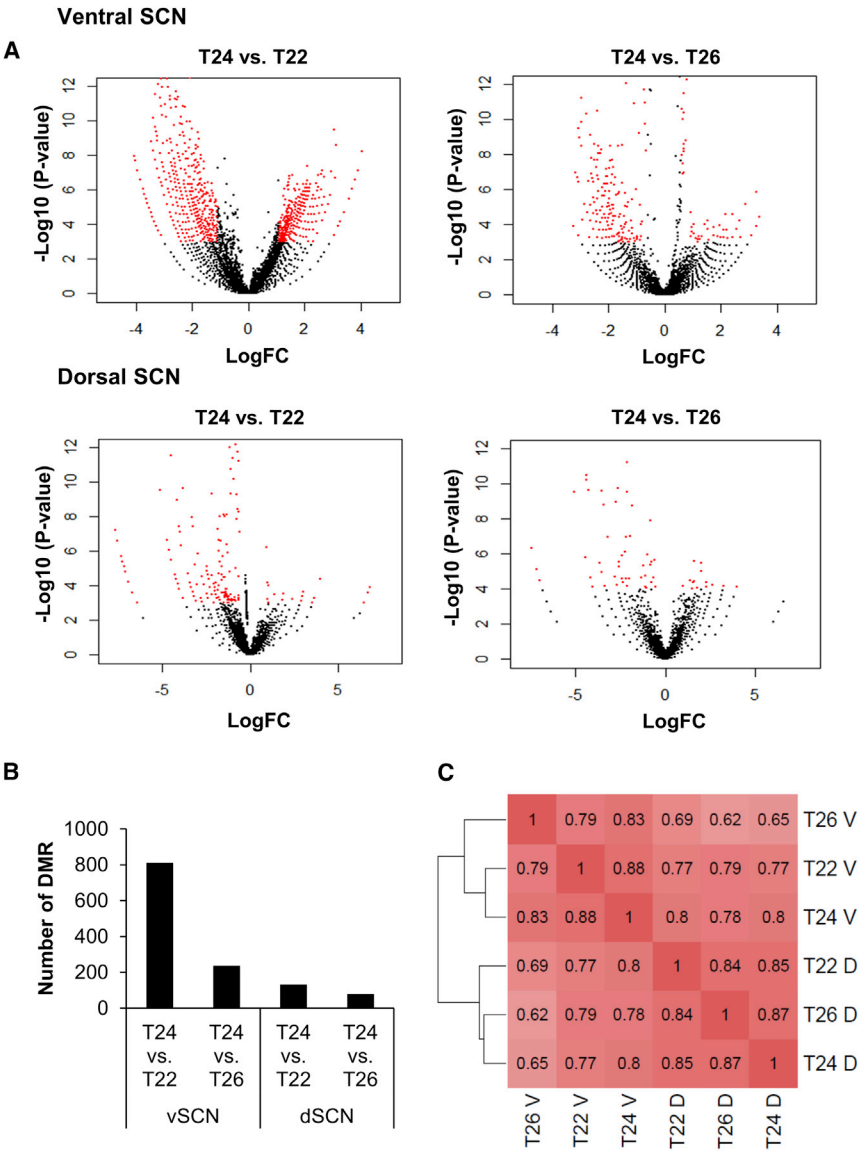

Figure 2. Different Light:Dark Cycle Lengths Drive Region-Specific Methylation Changes

See also Figures S4 and S5.

(A) Volcano plot depicting differentially methylated regions (DMRs). DMRs between the SCN sub-regions from different T-cycles are shown in red. Only MEDIP-sets with a least eight unique mapped reads used for the analysis were shown.

(B) Bar graph showing the number of DMRs between the SCN sub-regions.

(C) Correlation analysis of the methylation profiles between the SCN sub-regions from different T-cycles across refseq mouse genes (version mm9). Color and number indicate the correlation co-efficient (Pearson r), calculated via Liu et al. (2011).

and only the coupling signals sent by the vSCN oscillator are assumed to adapt to the photic condition. The detailed model is described in Supplemental Information. Modeling an intact SCN, the system exhibits a delayed phase of entrainment, with the core (vSCN) leading the shell (dSCN) under T22, and an after-effect of a shortened period (22.9 hr). Under T26, the shell (dSCN) precedes the core (vSCN) and displays an advanced phase of entrainment with a lengthened period (24.5 hr) upon release to constant darkness (Figure 5B), reproducing what is observed for mouse behavior in vivo (Figures 1A, 1B, and S1). By contrast, the model's simulation of an SCN explant (weighted sum of 30% core and 70% shell) shows the reverse: in effect, transient dynamics due to the reduced synchronization in the slice lead to an apparent lengthening of the period following T22 and shortening following T26 (Figure 5C), as observed in SCN slices (Figures 1C and 1D). The model also accurately anticipates the differences in relative phase (Figure 5B) and in SCN explant period (Figure 5D) that we observed when comparing T22, T24, and T26 conditions. These modeling results demonstrate that changes in global period length can be achieved by changes in coupling alone, without changing the intrinsic period of the underlying oscillators, and that complementary coupling signals may play an essential role in environmental adaptation.

From this model, a significant prediction also emerges: in particular, the desynchronizing coupling signal should play a critical role in the generation of period aftereffects, providing a counterbalance to the synchronizing signal to facilitate greater adaptability of the SCN network. Experimentally, it has long been known that that GABAergic signaling plays a critical role in maintaining phase relationships among SCN neurons (Albus et al., 2005) and that desynchronizing signals can be GABAergic (DeWoskin et al., 2015; Evans et al., 2013; Freeman et al., 2013a; Myung et al., 2015). Furthermore, the phase response curve for tonic GABA excitatory and inhibitory stimuli predicted by the detailed model of DeWoskin et al. (2015) supports the notion that excitatory neurotransmission may act as a synchronizing coupling function, while inhibitory neurotransmission may act as a desynchronizing coupling function, analogous to the complementary coupling mechanisms in our simple model.

To test the prediction that GABA signaling is necessary to maintain reverse period aftereffects in vitro, we cultured SCN slices from PER2::LUC mice exposed to T22, T24, and T26 in the presence or absence of the $GABA_A$ receptor antagonist gabazine (10 μM), which acts as an allosteric inhibitor (Ueno et al., 1997). Consistent with previous findings, gabazine had no effect on SCN period from T24 mice (Freeman et al., 2013b). However, gabazine treatment induced complete relaxation of SCN period from mice entrained to T22 and T26 back to T24 values (Figures 6A and 6B). Therefore, we conclude that

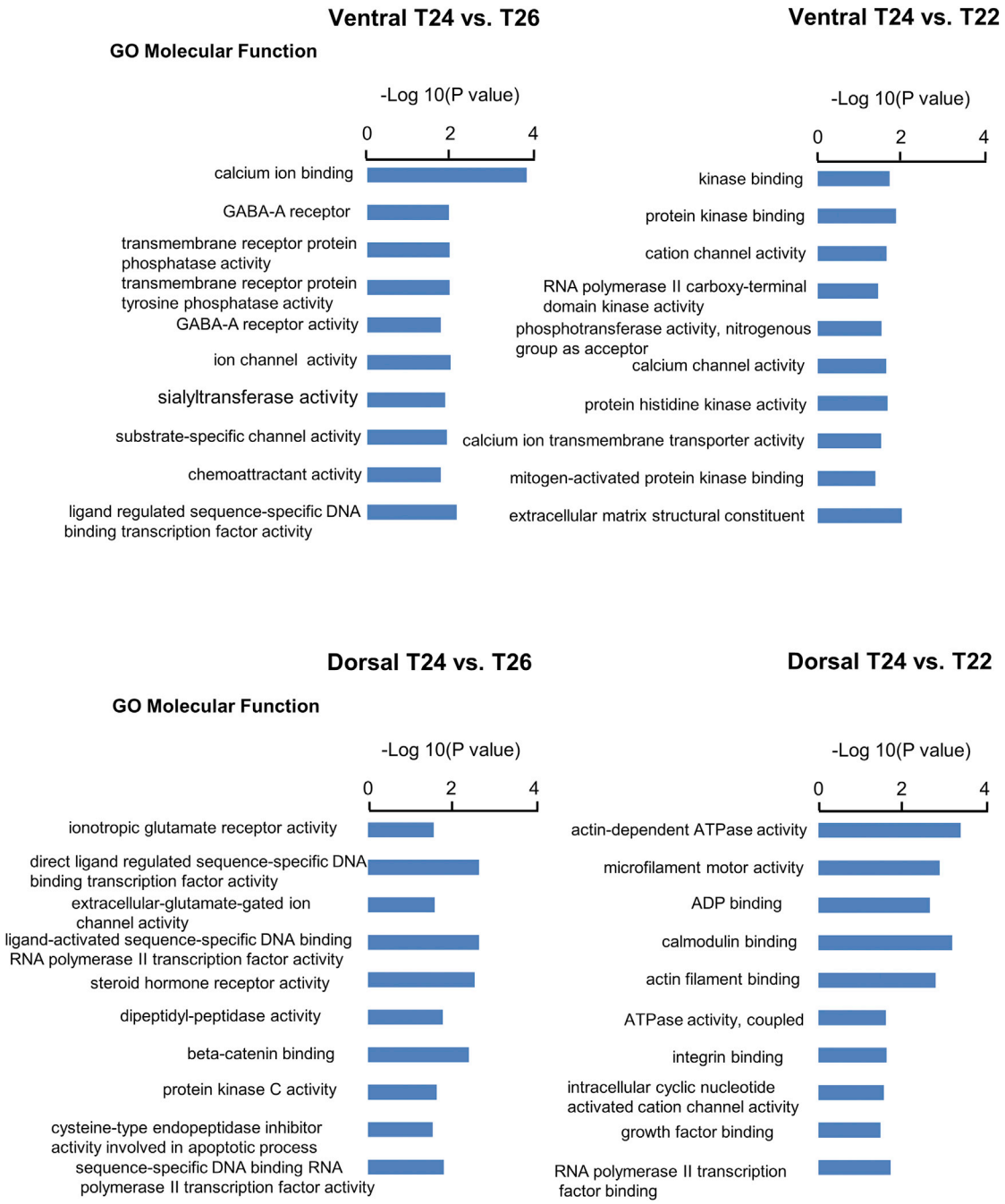

Figure 3. Pathways Affected by Light:Dark Cycle-Dependent Methylation

See also Figures S4 and S5. Negative Log of p value plot showing the top ten terms associated with molecular function of differentially methylation regions using the ENRICHR tool (Chen et al., 2013; Kuleshov et al., 2016).

GABAergic plasticity is necessary to maintain adaptation to light:dark cycle length.

DNA Methylation Is Necessary for Reverse Period Aftereffects In Vitro

Finally, if regional DNA methylation plays an important role in maintaining the SCN phase polarization that we observed, then it might be expected that inhibition of de novo DNA methylation would lead to relaxation of these changes and suppression of the reverse period aftereffects caused by SCN regional phase polarization. In fact, this is exactly what we observe: whereas treatment of SCN slices with zebularine (an inhibitor of DNA methylation) does not alter period in T24-entrained mice, treatment of slices from either T22- or T26-entrained

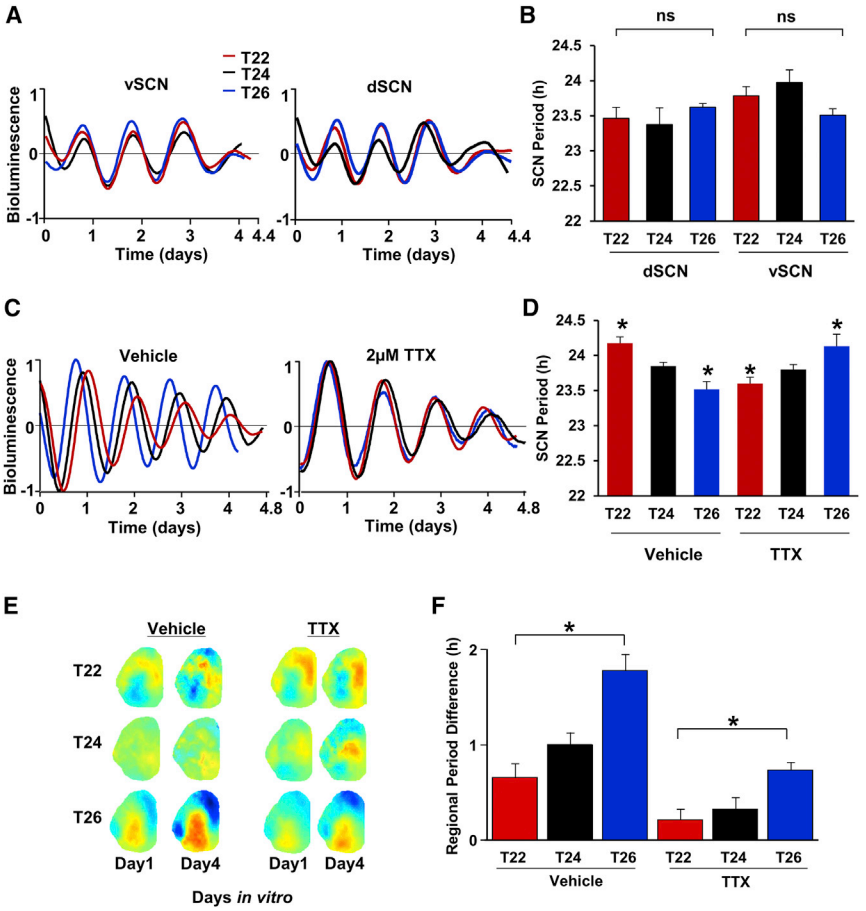

Figure 4. SCN Interregional Communication Drives Light:Dark Cycle Length-Dependent Period Changes

(A) PER2::LUC rhythms of separated vSCN and dSCN slices collected from T22, T24, and T26 mice.

(B) Bar graph showing period of separated vSCN and dSCN slices from T22, T24, and T26 mice. (n = 8–9 mice/group). dSCN: 1w-ANOVA F (2,22) = 0.543, p = 0.58); vSCN: 1w-ANOVA F(2,22) = 2.826, p = 0.08.

(C) PER2::LUC rhythms of SCN slices from mice entrained to different light:dark cycle lengths with and without 2 μM TTX.

(D) Bar graph showing period of data from (C) (n = 6–7 mice/group). Vehicle: 1w-ANOVA F(2,15) = 13,269 p < 0.0001, * Dunnett's post hoc test, p < 0.05; TTX: 1w-ANOVA F (2,15) = 5.249 p < 0.05; * Dunnett's post hoc test, T22 versus T26 p < 0.05.

(E) Average phase maps of PER2::LUC bioluminescence of SCN slices from mice entrained to different light:dark cycle lengths, with or without 2 μM TTX. n = 8 mice/group. Color scale as in Figure 1E.

(F) Quantification of regional period differences for SCN slices cultured with or without 2 μM TTX. y axis, period of the dSCN subtracted from the period of the vSCN. Statistics–Vehicle: 1w-ANOVA F(2,28) = 11.28, p < 0.0001; TTX: 1w-ANOVA F(2,28) = 5.22, p < 0.05; * Tukey's HSD test, p < 0.05. Errors bars are mean ± SE.

mice results in relaxation of their circadian period toward 24 hr (Figures 6C and 6D).

DISCUSSION

Within the circadian system, many environmental influences act directly upon components of the cellular molecular clockwork. For example, light cues induce expression of PER proteins (Gau et al., 2002; Oster et al., 2003), and metabolic cues activate sirtuins (Asher and Schibler, 2011; Nakahata et al., 2008). We show here that light:dark cycle length can stably alter circadian clock period epigenetically, not by modifying the intrinsic properties of cellular clocks, but by spatiotemporal reorganization of the SCN neural network.

SCN region-specific changes in the timing of clock gene expression have been documented previously (Evans et al., 2013; Inagaki et al., 2007; Myung et al., 2015). These works focused upon photoperiod as a model system, varying the amount of light and darkness within the 24 hr day. As in this paper, the authors of these studies demonstrated that short or long photoperiod modulates regional phase polarization within the SCN. Further, different cell populations along the antero-posterior SCN axis tracked light onset or offset (Inagaki et al., 2007), much as ventral regions tracked T cycles in our study. Crucially, however, photoperiodic changes do not induce significant or long-lasting period aftereffects (Pittendrigh and Daan, 1976), suggesting that the mechanisms maintaining these network reorganizations might be different from those we characterize here.

Similar to manipulating light:dark length, however, these other paradigms established a strong role for GABA in maintaining phase relationships among SCN neurons (Albus et al., 2005; DeWoskin et al., 2015; Evans et al., 2013; Freeman et al., 2013a; Myung et al., 2015). Indeed, in seasonal timing, the polarity of postsynaptic currents induced by GABA may be an important determining factor (Evans et al., 2013; Farajnia et al., 2014; Myung et al., 2015). In other paradigms such as photoperiod, roles for additional coupling mechanisms such as neuropeptides like VIP (vasoactive intestinal polypeptide) have also been supported (Evans et al., 2013). For light:dark cycle length, independent roles for different synaptic and neuropeptidergic coupling modalities will require additional studies.

Fascinatingly, our data suggest that changes in coupling and regional phase themselves can alter circadian period. The plausibility of such a mechanism is shown not only by our own model, but also by other theoretical frameworks (DeWoskin et al., 2015; Herzog et al., 2004; Oda and Friesen, 2002). The overall picture that emerges is one in which cycle length epigenetically reprograms DNA methylation in the SCN. These modifications in turn lead to a change in coupling, triggering the network to reorganize to find a new

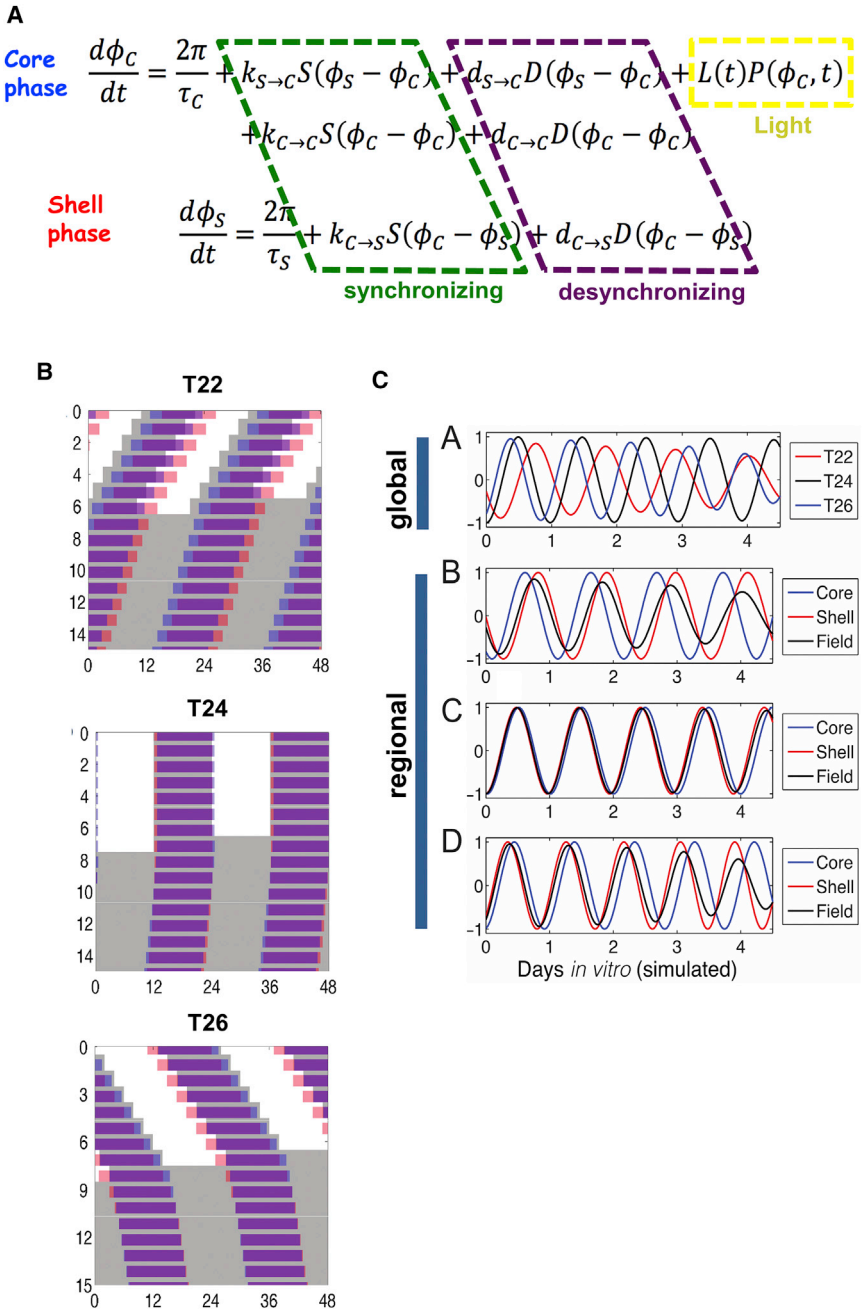

Figure 5. Modeling Predicts that GABAergic Signaling Is Necessary for Light:Dark Cycle Length-Dependent Period Changes

See also Figure S6.

(A) Our model consists of two coupled phase-only oscillators, representing the core (vSCN) and shell (dSCN) regions of the SCN. The core region has intrinsic period τ_C and phase ϕ_C, while the shell region has intrinsic period τ_S and phase ϕ_S. The coupling between the core and shell is composed of two complementary mechanisms that depend on the difference in phase: a synchronizing signal $S(\Delta\phi)$ and a signal $D(\Delta\phi)$ that in some situations tends to de-synchronize phases.

(B) Actograms of model simulations of whole SCN entrained to T22 (left), T24 (middle), and T26 (right) conditions, followed by aftereffects in constant darkness, which correspond to the preceding cycle lengths. Darkness is indicated in gray. Blue indicates subjective night (CT12–CT24) of the core oscillator (vSCN) and red shows subjective night of the shell oscillator (dSCN), with overlap appearing purple.

(C) Simulations of SCN explant rhythms under different light:dark cycle lengths. y axis, relative amplitude of summed components. (A) The simulated field rhythms are a weighted sum of core (30%) and shell (70%) and exhibit reversed aftereffects on period. Core, shell, and field rhythms of a simulated SCN slice are also shown following entrainment to (B) T22, (C) T24, and (D) T26. See Figure S6 for period values.

phase and period equilibrium. In this way, changes in network topology result in changes to basic clock properties like period length.

Input-dependent changes to the firing properties of neural circuits are essential to most aspects of brain function, including cognitive and emotional processing (Malenka and Bear, 2004). Our results show that neuroadaptations in the circadian clock in fact coopt some of these same paradigms. Moreover, although the processes that drive circadian timing and memory are quite different, the data we present suggest that essential characteristics of the adaptive process may be identical: DNA methylation has been shown to be important not only for stable responses of the circadian clock to environmental change (Azzi et al., 2014; Stevenson and Prendergast, 2013), but also for long-term memory (Zovkic et al., 2013) and for changes in adult behavior as a consequence of maternal care (Weaver et al., 2004). Thus, the process of environmental adaptation via first epigenetic changes and then circuit-level reorganization to elicit behavioral change may be a universal feature of the process of neuroadaptation that is conserved across a wide range of behavioral processes.

EXPERIMENTAL PROCEDURES

For further information, see Supplemental Experimental Procedures.

Animals

Details of strains and husbandry are available online. In brief, male PER2::LUC mice (Yoo et al., 2004) 4–6 weeks of age were exposed to one of the three lighting conditions: a standard 24 hr cycle (abbreviated T24) with 12 hr of light and 12 hr of darkness (LD 12:12), a short 22 hr cycle with LD 11:11 (T22), or a long

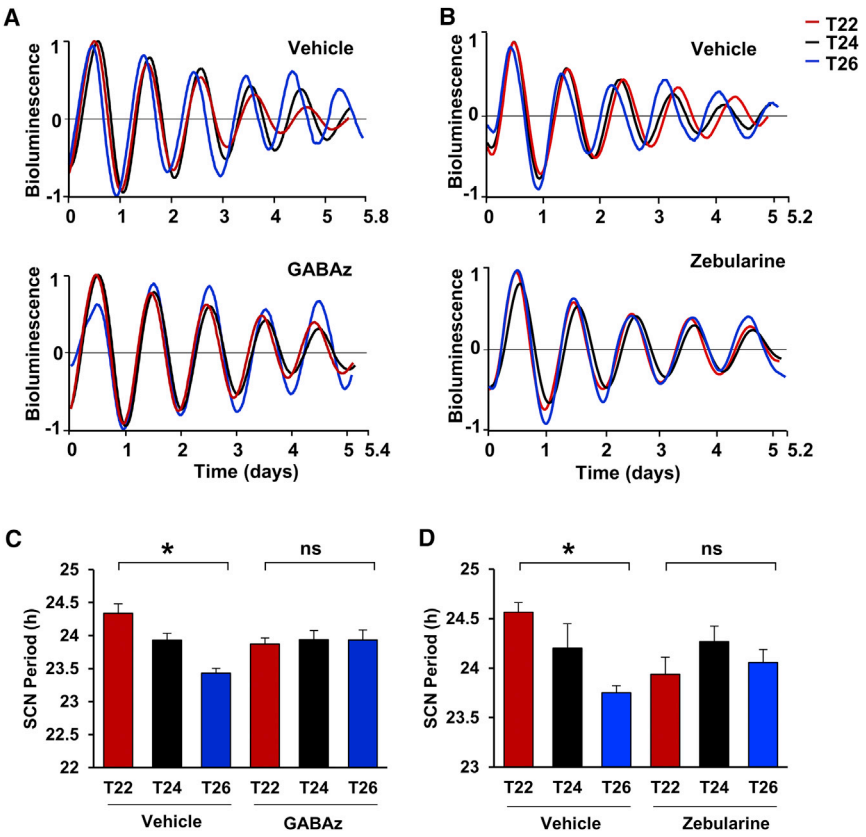

Figure 6. GABAergic Signaling and DNA Methylation Are Necessary for Light:Dark Cycle-Dependent Period Changes

(A) PER2::LUC rhythms of SCN slices from mice entrained to different light:dark cycle lengths with or without 10 μM gabazine (GABAz).

(B) Bar graph showing period of data from (A), n = 7–10 mice/group. Vehicle: 1w-ANOVA $F(2,24) = 12.417$, $p < 0.0001$; GABAz: 1w-ANOVA $F(2,25) = 0.083$, $p = 0.92$; * Dunnett's post hoc test, $p < 0.05$.

(C) PER2::LUC rhythms of SCN slices from mice entrained to different light:dark cycle lengths with or without 50 μM Zebularine.

(D) Bar graph showing period of data from (c), n = 6–16 mice/group. Vehicle: 1w-ANOVA $F(2,23) = 17.13$, $p < 0.0001$; Zebularine: 1w-ANOVA $F(2,25) = 1.07$, $p = 0.35$; * Dunnett's post hoc test, $p < 0.05$. Errors bars are mean ± SE.

26 hr cycle with LD 13:13 (T26). After 6 weeks, mice were either sacrificed immediately or released into constant darkness (DD) for 5–7 days to verify altered free-running period, prior to tissue collection. All animal experiments were conducted in accordance with applicable veterinary law of the Zurich cantonal veterinary office and the NIH Guide for the Care and Use of Animals. Experiments were approved by the Zurich cantonal veterinary office and Institutional Animal Care and Use Committee of Morehouse School of Medicine.

SCN Cultures

For luminometry experiments, one coronal SCN slice (~250 μm) was collected from the middle part of the SCN. For SCN imaging, three consecutive slices (150 μm thickness) were collected corresponding to the rostral, middle, and caudal SCN. Liver was excised and trimmed by hand with a scalpel. SCN and liver samples were cultured on a membrane (Millipore) in 1.2 mL medium containing 0.1 mM luciferin (Molecular Imaging Products, Bend, or Regies Technologies). For luminometry experiments, bioluminescence was collected in counts per minute for 5–6 days without medium change using a photomultiplier tube. For imaging experiments, SCN bioluminescence was monitored for at least 4 days using a Stanford Photonics XR Mega 10Z cooled intensified CCD camera and Piper software (Stanford Photonics). For drug treatments, tetrodotoxin (TTX; 2 μM, Tocris) or gabazine (GABAz; 10 μM, Tocris) were added to culture medium immediately upon dissection and remained in the culture medium for the duration of the recording.

Data Analysis

Wheel running rhythms were monitored and analyzed with the Clocklab data collection and analysis system (Actimetrics). Bioluminescence time series from photomultiplier tubes were analyzed with Lumicycle software (Actimetrics). For imaging data, PER2::LUC expression was mapped and analyzed using custom scripts in MATLAB 2014a (MathWorks), as described previously (Evans et al., 2011; Sellix et al., 2012). Briefly, SCN phase maps were generated for each 12-pixel diameter ROI judged to exhibit a significant circadian rhythm, and cell-like regions of interest (ROIs) were located and extracted after background and local noise subtraction. Behavioral and PER2::LUC data were analyzed with one way ANOVA followed by Dunnett's or Tukey's HSD post hoc tests. Data in figures and text are presented as mean ± SEM.

ACCESSION NUMBERS

The accession number for the MEDIP-seq data reported in this paper is GEO: GSE89255.

SUPPLEMENTAL INFORMATION

Supplemental Information includes Supplemental Experimental Procedures, Figures S1–S6, and Table S1 and can be found with this article online at http://dx.doi.org/10.1016/j.neuron.2016.12.022.

AUTHOR CONTRIBUTIONS

A.A., J.A.E., and J.M. performed the experiments; T.L. and J.A.E. performed the mathematical modeling and computational analysis. A.A., J.A.E., A.J.D., and S.A.B. contributed equally. A.A., J.A.E., T.L., J.M., T.T., A.J.D., and S.A.B. contributed both to experimental design and to writing this paper.

ACKNOWLEDGMENTS

A.A. has been supported by the Velux Foundation and the Forschungskredit of the University of Zürich. This work has received further support via S.A.B. from the Swiss National Science Foundation, the Velux Foundation, and the Clinical Research Priority Program "Sleep and Health" of the University of Zürich. A.A. and S.A.B. are members of the Zurich Neurozentrum, a division of the Life Sciences Zürich graduate program. J.A.E. was supported by R01NS091234. A.D.

was supported by NIH grants U54NS060659 and S21MD000101, the Georgia Research Alliance, and the NSF Center for Behavioral Neuroscience. T.L. gratefully acknowledges support through the Amherst College Faculty Research Award Program funded by The H. Axel Schupf '57 Fund for Intellectual Life. J.M. was supported by RIKEN Incentive Research Project (G1E-54500). J.M. appreciates partial support by Japan Society for Promotion of Science (JSPS) Grant-in-Aid (grant numbers 16H01652 and 16K08538). T.T. was supported by Ministry of Education, Culture, Sports, Science and Technology in Japan Grants-in-Aid for Scientific Research (25240277, 23111005, 26670165), Strategic International Cooperative Program from the Japan Science and Technology Agency, Intramural Research Grant for Neurological and Psychiatric Disorders of NCNP, and the Takeda Science Foundation. The authors would like to thank Oscar Cervantes-Castanon and Stanford Photonics for assistance.

Received: October 22, 2015
Revised: September 1, 2016
Accepted: December 9, 2016
Published: January 5, 2017

REFERENCES

Abraham, U., Granada, A.E., Westermark, P.O., Heine, M., Kramer, A., and Herzel, H. (2010). Coupling governs entrainment range of circadian clocks. Mol. Syst. Biol. *6*, 438.

Albus, H., Vansteensel, M.J., Michel, S., Block, G.D., and Meijer, J.H. (2005). A GABAergic mechanism is necessary for coupling dissociable ventral and dorsal regional oscillators within the circadian clock. Curr. Biol. *15*, 886–893.

Antle, M.C., and Silver, R. (2005). Orchestrating time: arrangements of the brain circadian clock. Trends Neurosci. *28*, 145–151.

Aschoff, J., and Pohl, H. (1978).). Phase relations between a circadian rhythm and its zeitgeber within the range of entrainment. Naturwissenschaften *65*, 80–84.

Asher, G., and Schibler, U. (2011). Crosstalk between components of circadian and metabolic cycles in mammals. Cell Metab. *13*, 125–137.

Aton, S.J., and Herzog, E.D. (2005). Come together, right...now: synchronization of rhythms in a mammalian circadian clock. Neuron *48*, 531–534.

Aton, S.J., Block, G.D., Tei, H., Yamazaki, S., and Herzog, E.D. (2004). Plasticity of circadian behavior and the suprachiasmatic nucleus following exposure to non-24-hour light cycles. J. Biol. Rhythms *19*, 198–207.

Aton, S.J., Colwell, C.S., Harmar, A.J., Waschek, J., and Herzog, E.D. (2005). Vasoactive intestinal polypeptide mediates circadian rhythmicity and synchrony in mammalian clock neurons. Nat. Neurosci. *8*, 476–483.

Azzi, A., Dallmann, R., Casserly, A., Rehrauer, H., Patrignani, A., Maier, B., Kramer, A., and Brown, S.A. (2014). Circadian behavior is light-reprogrammed by plastic DNA methylation. Nat. Neurosci. *17*, 377–382.

Brown, S.A., and Azzi, A. (2013). Peripheral circadian oscillators in mammals. Handbook Exp. Pharmacol. (217), 45–66.

Brown, S.A., Kunz, D., Dumas, A., Westermark, P.O., Vanselow, K., Tilmann-Wahnschaffe, A., Herzel, H., and Kramer, A. (2008). Molecular insights into human daily behavior. Proc. Natl. Acad. Sci. USA *105*, 1602–1607.

Chen, E.Y., Tan, C.M., Kou, Y., Duan, Q., Wang, Z., Meirelles, G.V., Clark, N.R., and Ma'ayan, A. (2013). Enrichr: interactive and collaborative HTML5 gene list enrichment analysis tool. BMC Bioinformatics *14*, 128.

DeWoskin, D., Myung, J., Belle, M.D., Piggins, H.D., Takumi, T., and Forger, D.B. (2015). Distinct roles for GABA across multiple timescales in mammalian circadian timekeeping. Proc. Natl. Acad. Sci. USA *112*, E3911–E3919.

Earnest, D.J., Digiorgio, S.M., and Sladek, C.D. (1991). Effects of tetrodotoxin on the circadian pacemaker mechanism in suprachiasmatic explants in vitro. Brain Res. Bull. *26*, 677–682.

Evans, J.A., Leise, T.L., Castanon-Cervantes, O., and Davidson, A.J. (2011). Intrinsic regulation of spatiotemporal organization within the suprachiasmatic nucleus. PLoS ONE *6*, e15869.

Evans, J.A., Leise, T.L., Castanon-Cervantes, O., and Davidson, A.J. (2013). Dynamic interactions mediated by nonredundant signaling mechanisms couple circadian clock neurons. Neuron *80*, 973–983.

Farajnia, S., van Westering, T.L., Meijer, J.H., and Michel, S. (2014). Seasonal induction of GABAergic excitation in the central mammalian clock. Proc. Natl. Acad. Sci. USA *111*, 9627–9632.

Freeman, G.M., Jr., Krock, R.M., Aton, S.J., Thaben, P., and Herzog, E.D. (2013a). GABA networks destabilize genetic oscillations in the circadian pacemaker. Neuron *78*, 799–806.

Freeman, G.M., Jr., Nakajima, M., Ueda, H.R., and Herzog, E.D. (2013b). Picrotoxin dramatically speeds the mammalian circadian clock independent of Cys-loop receptors. J. Neurophysiol. *110*, 103–108.

Gau, D., Lemberger, T., von Gall, C., Kretz, O., Le Minh, N., Gass, P., Schmid, W., Schibler, U., Korf, H.W., and Schütz, G. (2002). Phosphorylation of CREB Ser142 regulates light-induced phase shifts of the circadian clock. Neuron *34*, 245–253.

Hannibal, J., and Fahrenkrug, J. (2004). Target areas innervated by PACAP-immunoreactive retinal ganglion cells. Cell Tissue Res. *316*, 99–113.

Harmar, A.J., Marston, H.M., Shen, S., Spratt, C., West, K.M., Sheward, W.J., Morrison, C.F., Dorin, J.R., Piggins, H.D., Reubi, J.C., et al. (2002). The VPAC(2) receptor is essential for circadian function in the mouse suprachiasmatic nuclei. Cell *109*, 497–508.

Herzog, E.D., Takahashi, J.S., and Block, G.D. (1998). Clock controls circadian period in isolated suprachiasmatic nucleus neurons. Nat. Neurosci. *1*, 708–713.

Herzog, E.D., Aton, S.J., Numano, R., Sakaki, Y., and Tei, H. (2004). Temporal precision in the mammalian circadian system: a reliable clock from less reliable neurons. J. Biol. Rhythms *19*, 35–46.

Inagaki, N., Honma, S., Ono, D., Tanahashi, Y., and Honma, K. (2007). Separate oscillating cell groups in mouse suprachiasmatic nucleus couple photoperiodically to the onset and end of daily activity. Proc. Natl. Acad. Sci. USA *104*, 7664–7669.

Kriegsfeld, L.J., Korets, R., and Silver, R. (2003). Expression of the circadian clock gene Period 1 in neuroendocrine cells: an investigation using mice with a Per1:GFP transgene. Eur. J. Neurosci. *17*, 212–220.

Kuleshov, M.V., Jones, M.R., Rouillard, A.D., Fernandez, N.F., Duan, Q., Wang, Z., Koplev, S., Jenkins, S.L., Jagodnik, K.M., Lachmann, A., et al. (2016). Enrichr: a comprehensive gene set enrichment analysis web server 2016 update. Nucleic Acids Res. *44* (W1), W90-7.

Liu, C., Weaver, D.R., Strogatz, S.H., and Reppert, S.M. (1997). Cellular construction of a circadian clock: period determination in the suprachiasmatic nuclei. Cell *91*, 855–860.

Liu, A.C., Welsh, D.K., Ko, C.H., Tran, H.G., Zhang, E.E., Priest, A.A., Buhr, E.D., Singer, O., Meeker, K., Verma, I.M., et al. (2007). Intercellular coupling confers robustness against mutations in the SCN circadian clock network. Cell *129*, 605–616.

Liu, T., Ortiz, J.A., Taing, L., Meyer, C.A., Lee, B., Zhang, Y., Shin, H., Wong, S.S., Ma, J., Lei, Y., et al. (2011). Cistrome: an integrative platform for transcriptional regulation studies. Genome Biol. *12*, R83.

Lokshin, M., LeSauter, J., and Silver, R. (2015). Selective Distribution of Retinal Input to Mouse SCN Revealed in Analysis of Sagittal Sections. J. Biol. Rhythms *30*, 251–257.

Low-Zeddies, S.S., and Takahashi, J.S. (2001). Chimera analysis of the Clock mutation in mice shows that complex cellular integration determines circadian behavior. Cell *105*, 25–42.

Lowrey, P.L., Shimomura, K., Antoch, M.P., Yamazaki, S., Zemenides, P.D., Ralph, M.R., Menaker, M., and Takahashi, J.S. (2000). Positional syntenic cloning and functional characterization of the mammalian circadian mutation tau. Science *288*, 483–492.

Malenka, R.C., and Bear, M.F. (2004). LTP and LTD: an embarrassment of riches. Neuron *44*, 5–21.

Marsden, W.N. (2013). Synaptic plasticity in depression: molecular, cellular and functional correlates. Prog. Neuropsychopharmacol. Biol. Psychiatry *43*, 168–184.

Molyneux, P.C., Dahlgren, M.K., and Harrington, M.E. (2008). Circadian entrainment aftereffects in suprachiasmatic nuclei and peripheral tissues in vitro. Brain Res. *1228*, 127–134.

Myung, J., Hong, S., Hatanaka, F., Nakajima, Y., De Schutter, E., and Takumi, T. (2012). Period coding of Bmal1 oscillators in the suprachiasmatic nucleus. J. Neurosci. *32*, 8900–8918.

Myung, J., Hong, S., DeWoskin, D., De Schutter, E., Forger, D.B., and Takumi, T. (2015). GABA-mediated repulsive coupling between circadian clock neurons in the SCN encodes seasonal time. Proc. Natl. Acad. Sci. USA *112*, E3920–E3929.

Nagano, M., Adachi, A., Nakahama, K., Nakamura, T., Tamada, M., Meyer-Bernstein, E., Sehgal, A., and Shigeyoshi, Y. (2003). An abrupt shift in the day/night cycle causes desynchrony in the mammalian circadian center. J. Neurosci. *23*, 6141–6151.

Nakahata, Y., Kaluzova, M., Grimaldi, B., Sahar, S., Hirayama, J., Chen, D., Guarente, L.P., and Sassone-Corsi, P. (2008). The NAD+-dependent deacetylase SIRT1 modulates CLOCK-mediated chromatin remodeling and circadian control. Cell *134*, 329–340.

Nakajima, Y., Yamazaki, T., Nishii, S., Noguchi, T., Hoshino, H., Niwa, K., Viviani, V.R., and Ohmiya, Y. (2010). Enhanced beetle luciferase for high-resolution bioluminescence imaging. PLoS ONE *5*, e10011.

Nakamura, W., Yamazaki, S., Takasu, N.N., Mishima, K., and Block, G.D. (2005). Differential response of Period 1 expression within the suprachiasmatic nucleus. J. Neurosci. *25*, 5481–5487.

Nishide, S.Y., Honma, S., Nakajima, Y., Ikeda, M., Baba, K., Ohmiya, Y., and Honma, K. (2006). New reporter system for Per1 and Bmal1 expressions revealed self-sustained circadian rhythms in peripheral tissues. Genes Cells *11*, 1173–1182.

Noda, M., Ikeda, T., Suzuki, H., Takeshima, H., Takahashi, T., Kuno, M., and Numa, S. (1986). Expression of functional sodium channels from cloned cDNA. Nature *322*, 826–828.

Oda, G.A., and Friesen, W.O. (2002). A model for "splitting" of running-wheel activity in hamsters. J. Biol. Rhythms *17*, 76–88.

Oster, H., Werner, C., Magnone, M.C., Mayser, H., Feil, R., Seeliger, M.W., Hofmann, F., and Albrecht, U. (2003). cGMP-dependent protein kinase II modulates mPer1 and mPer2 gene induction and influences phase shifts of the circadian clock. Curr. Biol. *13*, 725–733.

Pendergast, J.S., Friday, R.C., and Yamazaki, S. (2010). Distinct functions of Period2 and Period3 in the mouse circadian system revealed by in vitro analysis. PLoS ONE *5*, e8552.

Pittendrigh, C.S., and Daan, S. (1976). A functional analysis of circadian pacemakers in nocturnal rodents. I. The stability and lability of of spontaneous frequency. J. Comp. Physiol. A Neuroethol. Sens. Neural Behav. Physiol. *106*, 223–252.

Ralph, M.R., Foster, R.G., Davis, F.C., and Menaker, M. (1990). Transplanted suprachiasmatic nucleus determines circadian period. Science *247*, 975–978.

Scheer, F.A., Wright, K.P., Jr., Kronauer, R.E., and Czeisler, C.A. (2007). Plasticity of the intrinsic period of the human circadian timing system. PLoS ONE *2*, e721.

Sellix, M.T., Evans, J.A., Leise, T.L., Castanon-Cervantes, O., Hill, D.D., DeLisser, P., Block, G.D., Menaker, M., and Davidson, A.J. (2012). Aging differentially affects the re-entrainment response of central and peripheral circadian oscillators. J. Neurosci. *32*, 16193–16202.

Stevenson, T.J., and Prendergast, B.J. (2013). Reversible DNA methylation regulates seasonal photoperiodic time measurement. Proc. Natl. Acad. Sci. USA *110*, 16651–16656.

Stokkan, K.A., Yamazaki, S., Tei, H., Sakaki, Y., and Menaker, M. (2001). Entrainment of the circadian clock in the liver by feeding. Science *291*, 490–493.

Toh, K.L., Jones, C.R., He, Y., Eide, E.J., Hinz, W.A., Virshup, D.M., Ptácek, L.J., and Fu, Y.H. (2001). An hPer2 phosphorylation site mutation in familial advanced sleep phase syndrome. Science *291*, 1040–1043.

Ueno, S., Bracamontes, J., Zorumski, C., Weiss, D.S., and Steinbach, J.H. (1997). Bicuculline and gabazine are allosteric inhibitors of channel opening of the GABAA receptor. J. Neurosci. *17*, 625–634.

Weaver, I.C., Cervoni, N., Champagne, F.A., D'Alessio, A.C., Sharma, S., Seckl, J.R., Dymov, S., Szyf, M., and Meaney, M.J. (2004). Epigenetic programming by maternal behavior. Nat. Neurosci. *7*, 847–854.

Yoo, S.H., Yamazaki, S., Lowrey, P.L., Shimomura, K., Ko, C.H., Buhr, E.D., Siepka, S.M., Hong, H.K., Oh, W.J., Yoo, O.J., et al. (2004). PERIOD2:LUCIFERASE real-time reporting of circadian dynamics reveals persistent circadian oscillations in mouse peripheral tissues. Proc. Natl. Acad. Sci. USA *101*, 5339–5346.

Zovkic, I.B., Guzman-Karlsson, M.C., and Sweatt, J.D. (2013). Epigenetic regulation of memory formation and maintenance. Learn. Mem. *20*, 61–74.